Chapter 8

# Heteroatom-Doped Graphene-Based Hybrid Materials for Hydrogen Energy Conversion

Bhaghavathi Parambath Vinayan

Additional information is available at the end of the chapter

http://dx.doi.org/10.5772/64242

## Abstract

Energy is becoming a big issue in the present world due to the depletion of current fossil fuels and also due to environmental problems such as global warming and rising pollution levels. Hence, highly efficient and renewable energy materials are required to produce clean electricity. The utilization of different energy sources such as solar energy and wind energy is hampered by their fluctuation in time and non-uniform geographical distribution which are still under nascent stage. In this regard, hydrogen-based renewable energy is very promising due to higher chemical energy per mass of hydrogen (142 MJ $kg^{-1}$) as compared to liquid hydrocarbons (47 MJ $kg^{-1}$), zero emission, and its large abundancy on earth. Therefore, electrochemical conversion of hydrogen to electric energy using fuel cells would be the key technology in future. In hydrogen fuel cells, the development of highly efficient electrocatalysts mainly for sluggish cathodic oxygen reduction reaction, with inexpensive and easily available materials, is a major issue. Recent investigations suggest that chemically modified graphene support materials such as nitrogen-doped graphene can generate strong, beneficial catalyst support interactions which considerably enhance the catalyst activity and stability in fuel cells. This chapter describes the fundamental aspects of electrochemical conversion of hydrogen to electric energy using fuel cells. The chapter further explains the role of nitrogen-doped graphene nanomaterials and their hybrids with transition metal and their alloy nanoparticles in fuel cell catalysis.

**Keywords:** graphene, nitrogen doping, hydrogen, fuel cells, alloy nanoparticles, oxygen reduction reaction

## 1. Introduction

In today's world, the rapid economic progress, increase in the population, and growing human dependence on energy appliances have led to a sharp increase in the global energy production and consumption that mainly originate from the non-renewable fossil fuels. This growing energy requirement imposes the urgency of newer sustainable, renewable, and environment friendly fuels. On this basis, the research and development of renewable energy resources and its conversion are of prime importance. The efficiency of renewable energy conversion devices mainly depend upon the structure and property of the active materials used in these devices. Recent research developments show that nanomaterials, particularly two-dimensional (2D) nanomaterials, such as graphene and its derivatives, can play a significant role in efficiency enhancement and performance of energy conversion and storage devices.

### 1.1. Development of graphene and its analogs

Graphene is a flat single layer of carbon atoms tightly packed into a 2D honeycomb lattice. Graphene can be considered as the fundamental building block of all graphitic materials with different dimensions. Graphene or graphene analogues can be synthesized mainly by bottom-up methods and top-down methods.

#### *1.1.1. Bottom-up synthesis methods*

One of the bottom-up approaches for the synthesis of single or few layer graphene is the chemical vapor deposition (CVD) method using the catalyst metal surfaces (Cu, Ni, Ir, Ru, etc.) and methane, acetylene, $CO_2$, or ethylene as the carbon source in the presence of argon or hydrogen. At high temperatures (~1000°C), pyrolysis of carbon precursor gas is taking place over the catalyst surfaces and single layer or few layer graphene is deposited on metal surfaces depending upon the heating rate, heating temperature, and flow rate of gases. Single-layer graphene with high structural quality were attained by low-pressure CVD of ethylene on a hot Ir(111) surface [1]. Recently, large single-crystalline graphene domains were grown by CVD on Ru(0001) using ethylene [2]. Large-scale graphene films can also be synthesized by CVD on polycrystalline nickel substrates [3]. Epitaxial growth is the other bottom-up strategy whereby a silicon carbide (SiC) substrate is heated to high temperatures (>1100°C) to form graphene [4]. In this method, growing of a single-layer graphene and achieving large graphene domains with uniform thickness remains a challenge. In CVD and epitaxial growth, the dimensions of the formed graphene mainly depend upon the size of the substrate, and at a time, one graphene layer only can be produced. Therefore, these methods are more suitable for microscale applications such as electronic or sensors and not suitable for applications where large amounts of materials are required such as energy related.

#### *1.1.2. Top-down synthesis methods*

In the top-down synthesis, methods of graphene consist of different methods such mechanical exfoliation of graphite, graphite intercalation methods, ultrasonic cleavage of graphite, oxidation, and subsequent exfoliation/reduction of graphite.

http://dx.doi.org/10.5772/64242

*(i) Mechanical exfoliation:* This is the best top-down synthesis method to get defect-free single-layer graphene, and this method involves the peeling of the layers of graphite using a scotch tape [5]. Different approach for the mechanical exfoliation is based on the concept of anodic bonding. In this method, at a particular temperature and voltage, graphite is sealed to a borosilicate glass and the subsequent peeling procedure gives a single- or few-layer graphene sheet on the substrate [6]. Scalability toward mass production and transfer of graphene sheets from the substrates are the major challenges in the mechanical exfoliations.

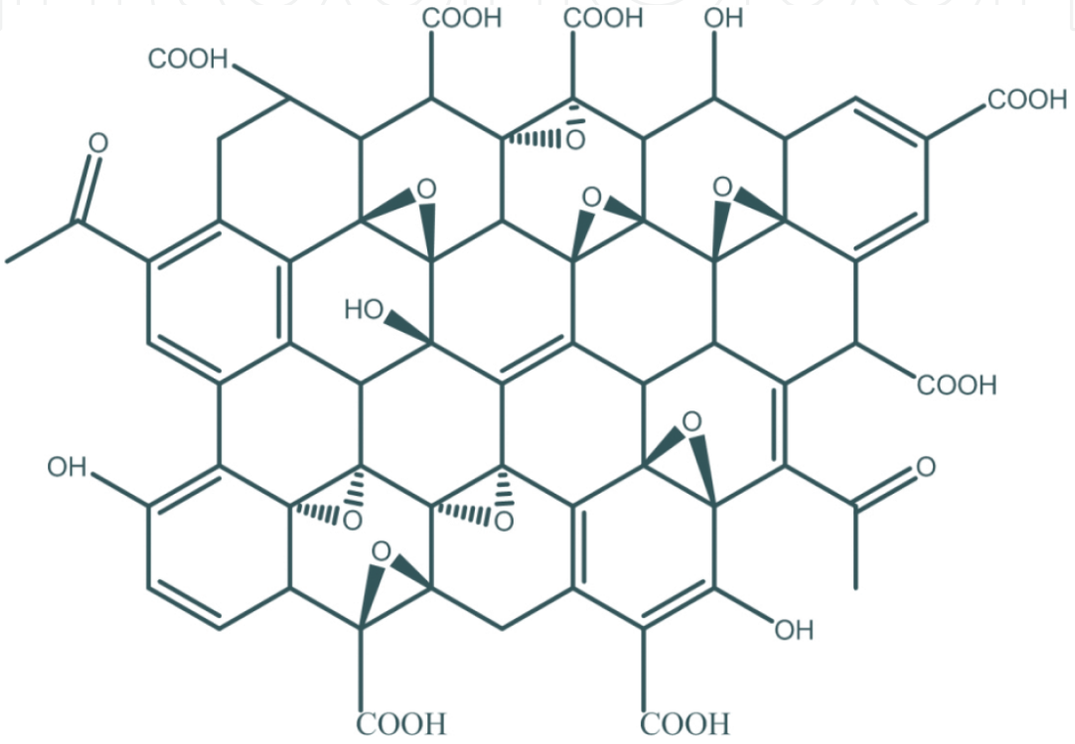


**Figure 1.** Schematic representation of the structure of graphite oxide.

*(ii) Graphite intercalation:* In this method, initially atoms or molecules such as alkali metal atoms (Li, Na, K, etc.) or acid (nitric acid, sulfuric acid, etc.) molecules are intercalated between the graphitic layers [7]. That weakens the Van der Waals interactions between the layers of graphite and facilitates the exfoliation or gives expanded graphite (EG) with partial oxidization. Giving a thermal shock at high temperatures (~1000°C) to EG provide graphite nanosheets or graphite nanoplatelets that contain multiple numbers of graphene layers (~10–50 layers).

*(iii) Ultrasonic cleavage method:* Here, graphite is initially suspended in particular organic solvents or surfactants (*N*-methyl-2-pyrroldinone,*N*,*N*-dimethylformamide, sodium dodecyl benzene sulfonate, etc.) and then gives an ultrasonic agitation to supply the energy to cleave the graphite [8]. The yield of getting single layer graphene at the first stages of this method is very low (~1 wt. %) and it can be increased by repeated sediment recycling. The success of

ultrasonic cleavage depends on the right selection of solvents and surfactants as well as the sonication frequency, amplitude, and time.

*(iv) Graphite oxide (GO)-reduction and exfoliation:* GO can be synthesized by the oxidative treatment of graphite via one of the following methods: Brodie [9], Staudenmaier [10], and Hummers [11]. Brodie's method was the addition of potassium chlorate ($KClO_3$) to the slurry of graphite in fuming nitric acid. Staudenmaier improved Brodie's method by adding the chlorate in multiple aliquots over the course of reaction in place of a single addition as Brodie had done. After that, Hummer found out an alternate oxidation method by reacting graphite with a mixture of potassium permanganate ($KMnO_4$) and concentrated sulfuric acid ($H_2SO_4$) [11]. The basal planes of GO are decorated with epoxide and hydroxyl groups, while edges are anchored with carboxyl and carbonyl groups as shown in **Figure 1**. Thus, GO consisting of layered structure of "graphene oxide" sheets with an interlayer spacing of ~0.84 nm. Completely oxidized GO is hydrophilic and an insulator due to the disruption of the $sp^2$-bonded carbon network. While partially oxidized GO is a semiconductor.

### *1.1.3. Chemical modifications of graphene-related nanomaterials*

Surface chemical modifications of graphene are necessary for making the composites with metals, polymers, alloys, etc., in relation to different energy applications. Carbon nanomaterials can be chemically modified by different methods such as covalent functionalization, non-covalent functionalization, and substitutional doping. In covalent functionalization, functional groups are attached to the carbon surface by the formation of covalent bond formation. This type of functionalization includes treating with oxidizing agents such as $H_2SO_4$, $HNO_3$, $KMnO_4$, $K_2Cr_2O_7$, polyphosphoric acid, and $H_2O_2$ that bring about the attachment of different oxygen functional groups such as hydroxyl (–OH), carboxyl (–COOH), and carbonyl (–C=O) over the surface of carbon nanostructures [12, 13]. In graphene-based materials, functionalization via acid treatments leads to the agglomeration of sheets and destruction of its novel properties like high surface area and electrical conductivity [14]. At the same time, non-covalent functionalization does not make any formal chemical bond formation between the foreign molecule and carbon surface, and this includes the attaching of various species of polymers [15], polynuclear aromatic compounds [16], surfactants [17], and biomolecules [18]. The non-covalent interaction is based on Van der Waals forces or π-π stacking interactions. Substitutional doping introduces heteroatoms, such as nitrogen atoms or boron atoms, into the carbon lattice of graphene, and this type of chemical modifications changes the electronic properties of carbon nanostructures. When a nitrogen atom is doped into graphene, it usually has three common bonding configurations within the carbon lattice, including quaternary N (or graphitic N), pyridinic N, and pyrrolic N as shown in **Figure 2** [19]. Pyridinic N bonds with two C atoms gives one p electron to the π system of graphene lattice. Pyrrolic N attributes to N atoms that donate two p electrons to the π system and bond with five-membered ring, like in pyrrole. N atoms that substitute for C atoms in the hexagonal ring are quaternary N. In these nitrogen types, pyridinic N and quaternary N are $sp^2$ hybridized, while pyrrolic N is $sp^3$ hybridized. In addition to these three usual nitrogen types, N oxides of pyridinic N have also been occasionally noticed in the nitrogen-doped graphene samples.

http://dx.doi.org/10.5772/64242

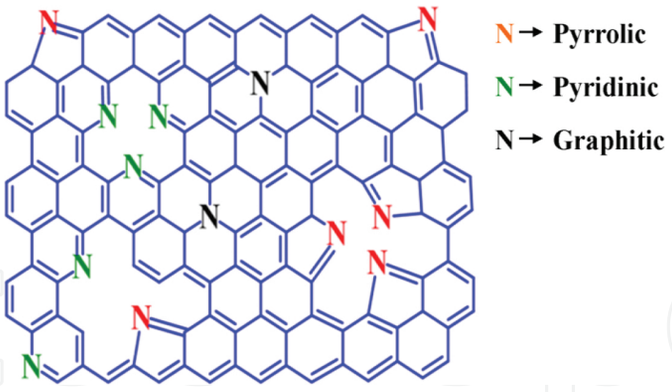


**Figure 2.** Schematic diagram of a nitrogen-doped graphene.

## 2. 2D nanomaterials for hydrogen energy conversion

### 2.1. Fuel cells

Fuel cells were discovered about 170 years ago by Sir William Grove. Fuel cell is a device that converts chemical energy into electrical energy. Usually electrochemical cells have two conductive electrodes called anode and cathode. The anode is defined as the electrode where oxidation occurs and the cathode is the electrode where the reduction takes place. Reactions at the anode (negative) usually take place at lower electrode potentials than that of the cathode (positive). Fuel cells are open systems, where the anode and cathode are just charge-transfer media and the active masses undergoing the redox reaction are delivered from outside the cell. To compare the power and energy densities of various electrochemical energy devices, a Ragone plot is used. The Ragone plot as shown in **Figure 3** illustrates that fuel cells can be considered as high-energy systems, whereas supercapacitors are considered to be high-power systems. Batteries have intermediate power and energy characteristics.

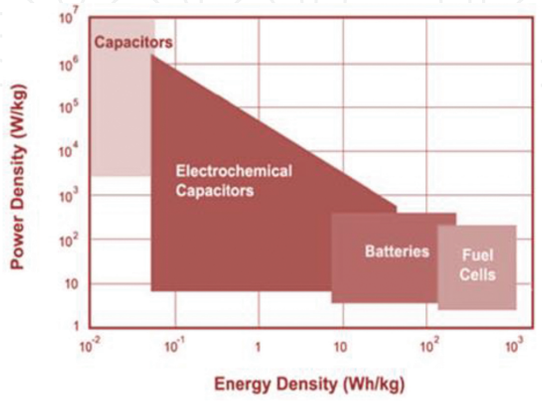


**Figure 3.** Ragone plot for different electrochemical energy devices [20].

### 2.2. Electrochemical aspects of fuel cells

The energy and power characteristics of fuel cells follow directly the thermodynamic and kinetic formulations for chemical reactions. The basic thermodynamics for a reversible electrochemical reaction is given by,

$$\Delta G = \Delta H - T\Delta S \tag{1}$$

Here $\Delta G$ is the Gibbs free energy, $\Delta H$ is the enthalpy, $\Delta S$ is the entropy, and $T$ is the absolute temperature, with $T\Delta S$ being the heat formed with the reaction. The terms, $\Delta G$, $\Delta H$, and $\Delta S$ are state functions and depend only on the identity of the electrode materials and the initial and final states of the reactions. The free energy $\Delta G$ represents the net useful energy available from a given reaction, thus, the net available electrical energy from a reaction in an electrochemical cell is given by,

$$\Delta G = -nFE \tag{2}$$

where $n$ is the number of electrons transferred per mol of reactants, $F$ is the Faraday constant (96,400 C $mol^{-1}$), and $E$ is the voltage of the cell with the specific chemical reaction. Eq. (2) represents a balance between the chemical and electric driving forces upon the ions under open circuit conditions; hence, $E$ refers to the open circuit potential of a cell where there is no current flowing. Since $\Delta G$ = -237 kJ $mol^{-1}$ under standard conditions for the reaction,

$$\mathrm{H_2} + \frac{1}{2}\mathrm{O_2} \rightarrow \mathrm{H_2O} \tag{3}$$

The reversible voltage for the hydrogen-oxygen fuel cell according to Eq. (2) is $E$ = 1.23 V.

The change of free energy ($\Delta G$) for a given species "$i$" defines the chemical potential ($\mu_i$). The chemical potential $\mu_i$ for species "$i$" is related to another thermodynamic quantity called chemical activity ($a_i$) by the defining relation:

$$\mu_i = \mu_i^o + RT \ln a_i \tag{4}$$

where $\mu_i^0$ is a constant, which is the value of the chemical potential of species "$i$" in its standard conditions, $R$ is the gas constant, and $T$ the absolute temperature.

Assume an electrochemical cell in which the activity of species "$i$" is distinctive in the two electrodes: $a_i(-)$ at the negative side and $a_i(+)$ at the positive side. The difference between the chemical potentials of positive and negative electrodes can be written as

http://dx.doi.org/10.5772/64242

$$\mu_i(+) - \mu_i(-) = RT \ln\left[\frac{a_i(+)}{a_i(-)}\right] \tag{5}$$

This chemical potential difference is balanced by the electrostatic energy from Eq. (2), then

$$E = E^0 - \frac{RT}{nF} \ln\left[\frac{a_i(+)}{a_i(-)}\right] \tag{6}$$

where $E^0$ is the voltage under standard conditions and this relation is called the Nernst equation, which relates the measurable cell voltage to the chemical differences across an electrochemical cell. If the activity of species "*i*" in one of the electrodes is a standard reference value, the Nernst equation provides the relative electrical potential of the other electrode.

Compared to the open circuit potential at equilibrium state, the voltage drops off when current is drawn from the electrochemical cell because of irreversible losses. If more current is withdrawn from the cell, greater the losses. **Figure 4** shows a typical discharge curve of a fuel cell. There are three major types of voltage losses in the discharge curve and that give its characteristic shape. These voltage losses are (i) activation losses due to electrochemical reaction kinetics ($\eta_{act}$), (ii) ohmic losses due to ionic and electronic resistances ($\eta_{ohmic}$), and (iii) concentration losses due to limited mass transport ($\eta_{conc}$). So, by subtracting all voltage losses from the thermodynamically predicted voltage output, the real voltage output of a fuel cell can be written as

$$V = E - \eta_{act} - \eta_{ohmic} - \eta_{conc} \tag{7}$$

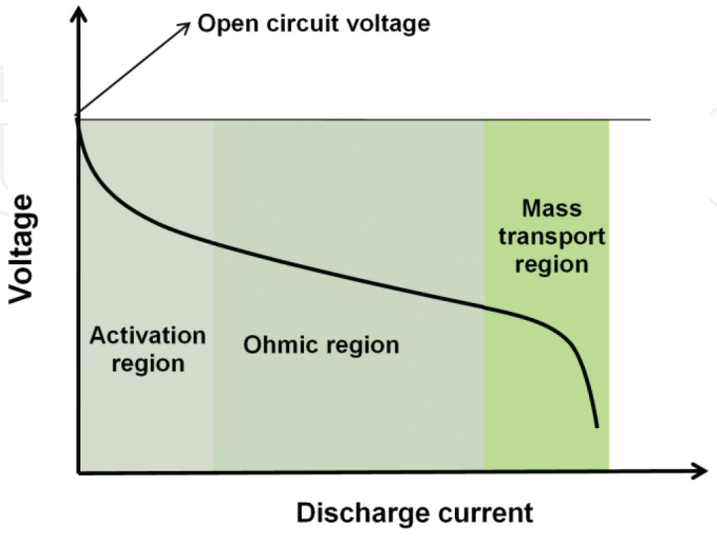


**Figure 4.** Discharge curve of a fuel cell.

### 2.3. Hydrogen fuel cells: working mechanism

Fuel cells can be classified primarily by the kind of electrolyte they employ; all of them work on the same principle. Different types of fuel cells are listed below:

- Polymer electrolyte membrane fuel cells (PEMFC)
- Alkaline fuel cells (AFC)
- Phosphoric acid fuel cells (PAFC)
- Molten carbonate fuel cells (MCFC)
- Solid oxide fuel cells (SOFC)

Among various types of fuel cell technologies, the PEMFC technology has received attention due to its high power density and efficiency (60–80%), relatively low operating temperature (less than 100°C), and the ability to respond quickly to the changing power demands. A schematic diagram of a PEMFC is given in **Figure 5(a)**. It comprises an anode, a cathode, and a polymer membrane as the proton-conducting media which separate both the electrodes. Hydrogen is supplied at the anode and oxygen is supplied at the cathode. Hydrogen oxidation is taking place at the anode and as a result, $H^+$ ions and electrons are produced. The $H^+$ ions are conducted through the proton exchange membrane and electrons through the external circuit to the cathode, where oxygen reduction reaction (ORR) is taking place and water and heat energy are produced as by-products. All the electrochemical reactions at the anode and cathode are taking place with the help of a catalyst only.

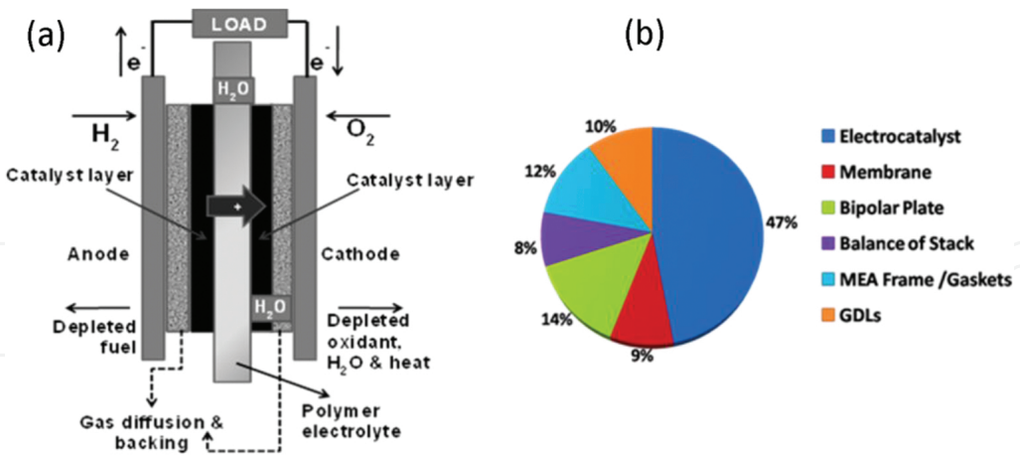


**Figure 5.** (a) Schematic illustration of a PEMFC. (b) Cost analysis of various fuel cell components. (Analysis data based on the US Department of Energy -Hydrogen Program Overview, 2008.)

The reactions taking place in PEMFC can be summarized as

$$\text{Anode}: \ 2H_2 \rightarrow 4H^+ + \ 4e^- \qquad \left(E^+ = \ 0.0 \text{ V vs. SHE}\right) \tag{8}$$

http://dx.doi.org/10.5772/64242

$$\text{Cathode}: 4H^+ + O_2 + 4e^- \rightarrow 2H_2O \left(E^- = 1.23 \text{ V vs. SHE}\right) \quad (9)$$

(SHE stands for standard hydrogen electrode)

The net reaction can be written as

$$H_2 + \tfrac{1}{2} O_2 \rightarrow H_2O \quad \left(E_{cell} = 1.23 \text{ V}\right) \quad (10)$$

### 2.4. Role of electrocatalysts in hydrogen fuel cells

For a wide-scale commercialization, the PEMFCs should overcome several challenges including two critical barriers, namely cost and durability. At present, platinum (Pt) is the best electrocatalyst in PEMFCs in light of the fact that it is adequately reactive at low temperatures for bonding with hydrogen and oxygen intermediates and catalyzes the electrode reactions to form the final products. Nevertheless, the high cost and insufficiency of Pt limit the practical implementations of PEMFC for static and automobile applications. **Figure 5(b)** shows the cost (in percentage) of different components within PEMFC. To date, 78% of the total cost of a fuel cell is due to the membrane electrode assembly of which 47% is contributed by the catalysts alone. At present, with the help of modern technology and nano materials, a PEMFC performance with maximum power densities of ≈1 W $cm^{-2}$ at the cell voltage of ≈ 0.65 V has been achieved using the Pt loading (anode and cathode) of 0.4–0.5 $mg_{Pt}$ $cm^{-2}$ [21, 22]. This PEMFC performance equals to fivefold reduction in the amount of Pt was used in the early of 2000. At present, the research world is looking for to reduce the Pt-specific power density lesser than that of 0.2 $g_{Pt}$ $kW^{-1}$ at the cell voltages of ≥0.65 V. According to the US department of energy (DOE), the key target is to reduce the fuel cell cost to $30/kW with 5000 h minimum durability. For reducing the PEMFC cost, the following approaches are implemented such as (i) alloying of Pt catalyst with 3d-transition metals (TM) to enhance the catalytic activity, (ii) maximum utilization of Pt by reducing the particle size and usage of proper catalyst support materials, and (iii) considerable reduction of mass-transport-induced voltage losses at high current densities with proper engineering of electrodes, diffusion media, and flow fields [21].

In PEMFC, sluggish kinetics of ORR causes a large over-potential at cathode side in low temperatures. Therefore, development of highly active cathode electrocatalysts is essential. Alloying Pt with 3d transition metals (TM), especially Co, Fe, Ni, and Cr, has been demonstrated to increase the ORR activity [23]. In particular, Pt-Co alloys have been found to exhibit enhanced catalytic activity toward the ORR [23–27]. The modified electronic structure of the Pt–TM alloy composite affects the Pt-Pt bond distance resulting in strong adsorption of the oxygen molecules and weak adsorption of ORR blocking $OH^-$ radicals over these alloy catalyst nanoparticles [23, 28]. In addition, it is essential to have a uniform dispersion and control over the size of catalyst particles for high activity [21, 29]. Metal catalyst nanoparticles have a very high tendency to agglomerate due to large metal-metal cohesion energy and which in turn leads to a decrease in the electrochemical surface area (ECSA). To sort out this issue, it is

important to search for a right catalyst supporting material that has a high surface area, excellent electronic conductivity, and strong affinity toward catalyst particles, on which a uniform dispersion of Pt NPs can be accomplished. Catalyst supports also take a role in altering the geometry and electronic properties of the catalysts particles during their growth. A highly conductive support can enable effective electron collection and their transfer to the collector electrode. It is required to have a good porosity in support materials for better mass transportation of the fuel and oxidant to the densely scattered triple phase boundaries. Carbon supports in presently using commercial platinum electrocatalysts (Pt/C) have a tendency of electrochemical oxidation during long-time operations in acidic environment, which leads to Pt nanoparticles agglomeration or detachment from the support material leading to the degradation of fuel cell performance [30].

### 2.5. Graphene-based fuel cell electrocatalysts

Since graphene is a two-dimensional planar sheet with open structure, there is the possibility of both sides of graphene being utilized for supporting the catalyst nanoparticles and which is expected to be a promising catalyst support material in the future. Graphite oxide is commonly used as the starting material for the bulk preparation of graphene-based fuel cell electrocatalysts. The various oxy functional groups over the surface of graphite oxide help for its dissolution in various solvents and serve as the anchors or nucleating centers for the controlled growth of catalyst nanoparticles on it. Different techniques have been reported for the decoration of platinum nanoparticles (Pt NPs) on graphene for fuel cell applications. Jafri et al. have synthesized graphene nanoplatelet-supported Pt NPs by reducing platinum chloride with $NaBH_4$ on thermally exfoliated graphene nanoplatelets [31]. Pt-graphene was also synthesized by in situ reduction of graphite oxide and platinum chloride using different polyol methods and $NaBH_4$ methods [32, 33]. In various synthesis methods of Pt-graphene, the dispersed nanoparticles exhibit a wide size range, a non-uniform spatial distribution, and the synthesis method does not provide significant control over the metal loading. This shows that the decoration of Pt NPs on graphene is a challenge in terms of controlling the particle size, distribution, and keeping the inherent properties of graphene such as high surface area and electronic conductivity intact. Therefore, the objectives of devising a synthesis method for Pt-graphene are related to fuel cell applications, which (a) yields high performance, (b) incurs low cost, (c) requires minimum resources, and (d) has optimum-sized catalyst particles (~3–5 nm) dispersed uniformly while preserving the inherent properties of graphene is of prime concern. Different graphene-based hybrid electrocatalyst materials such as graphene/Pt metal, graphene/Pt alloys, graphene/metal oxides, and heteroatom-doped graphene, etc. are effective in maximizing the ORR performance of PEMFC and have been illustrated in **Figure 6**.

The early reports of the PEMFC performance using Pt-graphene as ORR catalysts were not competitive with the commercial Pt/Vulcan carbon electrocatalysts. In the early studies, Seger et al. reported a maximum power density value of ~160 mW $cm^{-2}$ for Pt-graphene electrocatalyst as synthesized by $NaBH_4$ reduction method [32]. A fuel cell performance of ~350 mA $cm^{-2}$ at 0.6 V was shown by Si et al. for Pt-graphene cathode electrocatalyst [34]. The main reason for this comparatively lower performance is the decrease in the surface area due to restack-

http://dx.doi.org/10.5772/64242

ing of graphene sheets and poor electronic conductivity because of the inappropriate synthesis procedures.

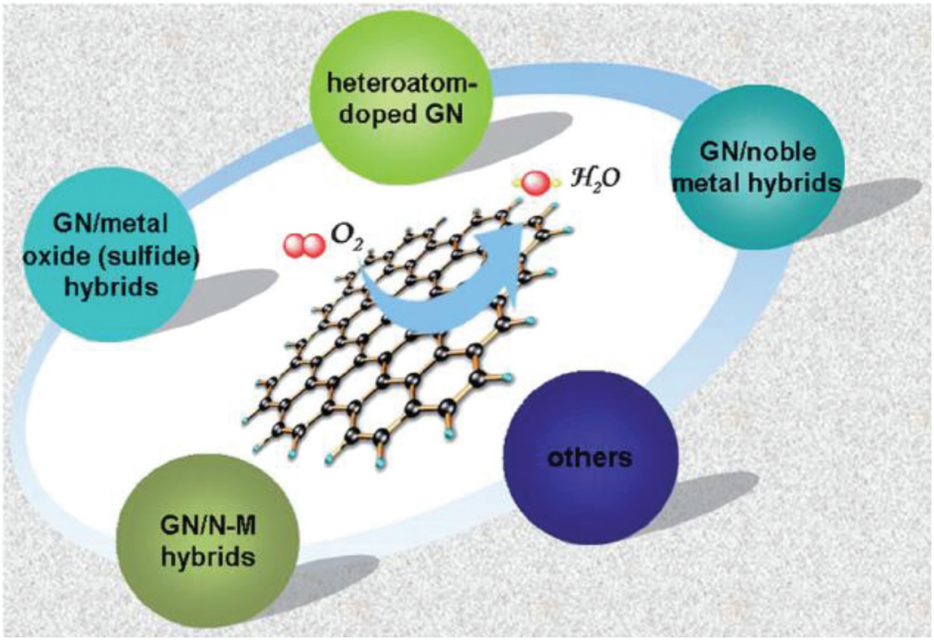


**Figure 6.** Various graphene-based nanomaterials as catalysts for ORR. (Reprinted from ref. [35] with permission of The Royal Society of Chemistry).

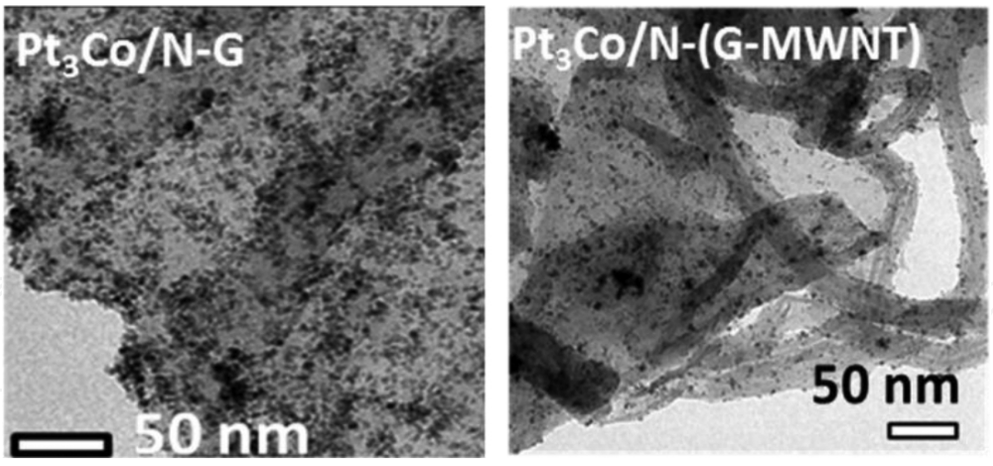


**Figure 7.** TEM image of $Pt_3Co$/nitrogen-doped graphene ($Pt_3Co$/NG), $Pt_3Co$/nitrogen-doped (graphene-MWNT) hybrid structure ($Pt_3Co$/N-(G-MWNT)) [25, 26].

To overcome the problem of restacking, incorporation of metal nanoparticles and nanotubes was used during the synthesis of graphene itself and these nanoparticles/nanotubes act as the spacers in between the graphene layers, which prevent further agglomeration of the sheets [36, 37]. Further to enhance the electrical conductivity and electrochemical activity of graphene, heteroatom doping (N, B, S, or P) is a very promising method [38–42].

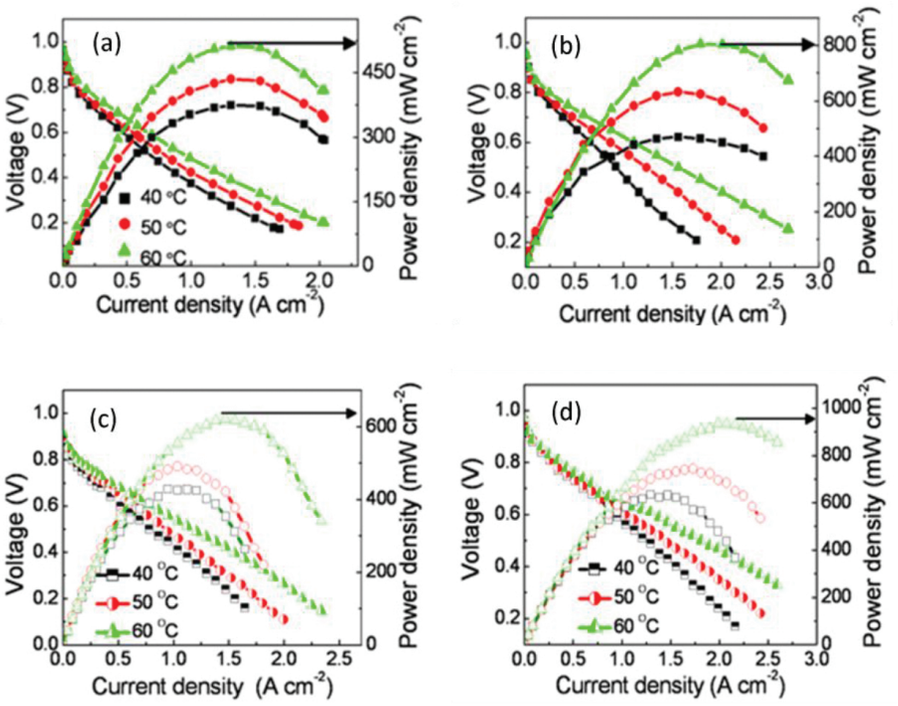


**Figure 8.** Polarization curves of cathode electrocatalysts (a) Pt/N-G, and (b) $P_3Co$/N-G, (c) Pt/N-(G-MWNT), and (d) $Pt_3Co$/N-(G-MWNT) with Pt/C as anode electrocatalyst at three different temperatures (40, 50, 60°C) without any back pressure [25, 26].

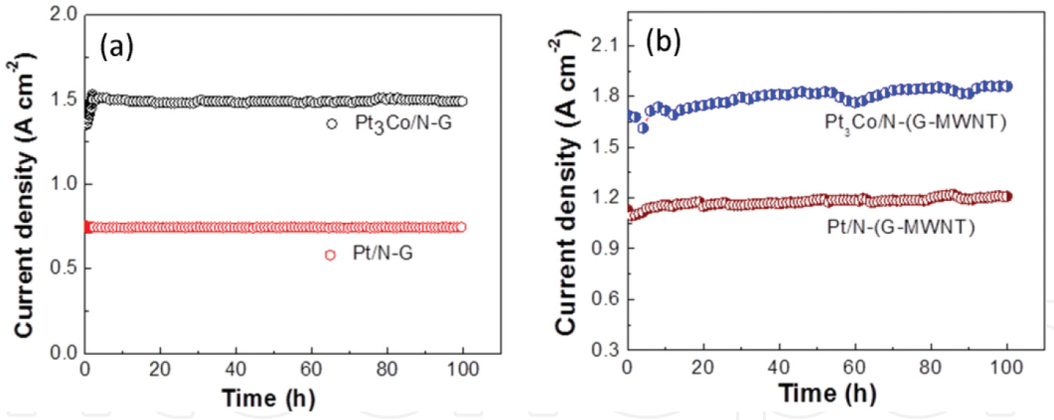


**Figure 9.** (a–b) Stability of PEMFC with (a) Pt/N-G, and (b) $P_3Co$/N-G, (c) Pt/N-(G-MWNT), and (d) $Pt_3Co$/N-(G-MWNT) as cathode electrocatalysts and Pt/C anode electrocatalyst at 0.5V in 60°C temperature with no back pressure [25, 26].

**Figure 7** illustrates the uniform distribution of $Pt_3Co$ alloy nanoparticles over the surface of nitrogen-doped graphene and graphene-multiwalled carbon nanotubes (MWNT) hybrid structures. The PEMFC performance polarization curves for Pt or $Pt_3Co$ alloy catalysts nanoparticle dispersed nitrogen-doped graphene (NG) and nitrogen-doped (graphene-MWNT) hybrid catalysts have been shown in **Figure 8**. The corresponding performance values of the electrocatalysts are summarized in **Table 1**. The commercial Pt/C was used as the anode

http://dx.doi.org/10.5772/64242

catalysts for all cathode catalysts. A catalyst loading of 0.25 and 0.4 $mg_{pt}$ $cm^{-2}$ were sustained at the anode and the cathode, respectively. **Figure 9(a)** and **(b)** compares the stability of the above electrocatalysts for 100 h at 0.5 V in 60°C temperature with no back pressure.

| Cathode electrocatalyst | ECSA ($m^2$ $g^{-1}$) | Temperature = 60°C | |
|---|---|---|---|
| | | Current density at 0.6 V (mA $cm^{-2}$) | Maximum power density (mW $cm^{-2}$) |
| Pt/N-G | 57.9 | 665 | 512 |
| $Pt_3Co$/N-G | 48.5 | 1110 | 805 |
| Pt/N-(G-MWNT) | 79.2 | 804 | 783 |
| $Pt_3Co$/N-(G-MWNT) | 98.5 | 1344 | 935 |

**Table 1.** PEMFC performance of Pt and $Pt_3Co$ alloy catalysts using nitrogen doped graphene.

The superior PEMFC performance exhibited by $Pt_3Co$/nitrogen-doped nano-carbon cathode electrocatalysts ($Pt_3Co$/N-G and $Pt_3Co$/N-(G-MWNT)) can be viewed from two perspectives as shown in **Figure 10**, that is (i) the catalytic activity of $Pt_3Co$ alloy nanoparticles and (ii) the role played by nitrogen doping in carbon support nanomaterials.

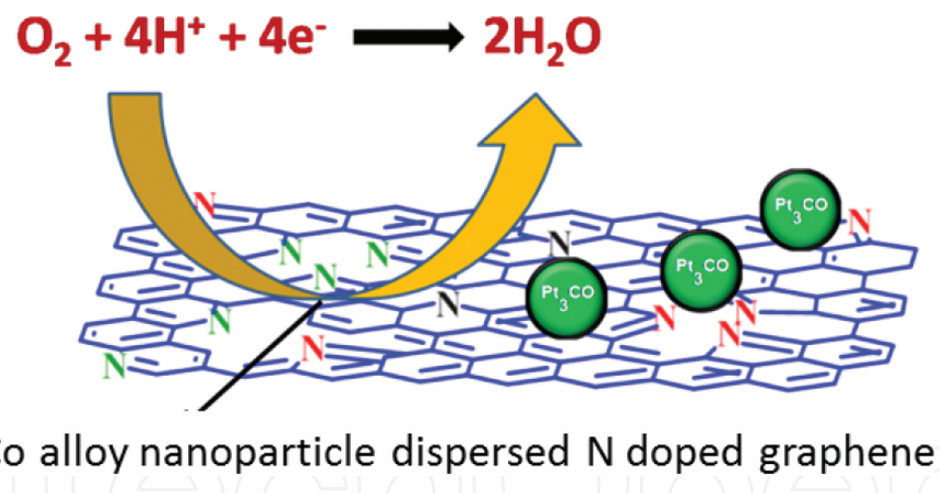


**Figure 10.** ORR in $Pt_3Co$ alloy nanoparticle dispersed nitrogen-doped graphene.

In ORR electrocatalysts, two opposing effects should counter balance each other such as comparatively strong adsorption energy of oxygen and ORR reaction intermediates ($O_2^-$, $O_2^{2-}$) and at the same time, low adsorption of ORR blocking species such as $OH^-$ anions and oxides [21]. For Pt metal surfaces the d-band center is closer to the Fermi level and they firmly adsorb both oxygen and ORR-blocking $OH^-$ species and that restricts the availability of free Pt sites for ORR [43]. There is a shift in Pt d-band center from Fermi level and a reduction of Pt-Pt bond distance can be created as a result of the alloying of Pt with transition metals [44]. Despite the fact that more shifts in d-band center from Fermi level makes a less adsorption of OH-species and at the same time the ORR rate is less because of the feeble adsorption of oxygen.

Consequently, the movement in d-band center ought to be ideal in a manner that to balance the solid adsorption of oxygen and weak adsorption by $OH^-$ blocking species. The shift in *d*-band center is optimum for $Pt_3TM$ (TM = Fe, Co, Ni) electrocatalysts in such a way that to give high ORR activity as compared to other Pt-TM alloys or pure Pt [45]. Also the uniform dispersion of catalyst particles with appropriate particle size (~3–5 nm) again enhances the ORR activity of the electrocatalysts.

The formation of an atomic charge density and asymmetry in spin density on nitrogen-doped graphene system encourages the charge exchange from the carbon support to the adsorbing oxygen molecule and results in the creation of an superoxide ion ($O_2^{\bullet -}$) [25, 46]. This debilitates the O–O bond and helps for its easy dissociation. In other words nitrogen doping helps for the $4e^-$ transfer reaction rather than $2e^-$ transfer reaction in ORR reaction [38]. Moreover, the doping of nitrogen atoms into the graphene lattice reinforces the bonding between the catalysts nanoparticles and the support that not just aides in a uniform dispersion of catalyst particles on the carbon support additionally prevents their self-agglomeration during long PEMFC operation [47]. In nitrogen-doped (graphene-MWNT) hybrid structures, the nitrogen doping also increases the electrical conductivity of graphene support materials along with highly conductive carbon nanotubes [25].

## 3. Future outlook and challenges

The gathering of many unique properties of graphene-related 2D nanomaterials such as large surface area, excellent conductivity, good mechanical, and chemical stability along with low cost and accessibility for mass production has opened up a new research area in the field of materials science. Chemical modification of graphene-related materials especially by nitrogen doping and incorporation of Pt and Pt alloys can significantly increase the catalytic activity and durability toward oxygen electro-reduction. Even though the following things need to be investigated in depth for future studies such as (a) the exact nature of electrocatalytically active sites facilitating the ORR in N-doped graphene and origin of their catalytic reactivity, (b) design of facile and large-scale synthesis approaches, for N-doped graphene and their hybrids with metals and alloy nanoparticles. With respect to N-doped graphene synthesis, the technique should be capable of the large incorporation of electrochemically active N functional groups to the support. Regarding N-doped graphene hybrids, the method should ensure the precise tuning of the size, morphology and compositions of electrocatalyst particles for getting high ORR catalytic activity and strong bonding between N-doped support and catalyst nanoparticles for long-term durability, and (c) investigation of alloying effect of Pt with 3d transition metals (Co, Fe, Ni, Cu, etc.) supported on N-doped graphene towards ORR by DFT modeling and electrochemical experiments.

## Acknowledgements

B.P. Vinayan acknowledges the Alexander von Humboldt Foundation for research funding.

## Author details

Bhaghavathi Parambath Vinayan

Address all correspondence to: vinayan.parambath@kit.edu

Helmholtz Institute Ulm for Electrochemical Energy Storage (HIU), Ulm, Germany

## References

[1] Coraux J, N'Diaye AT, Busse C, Michely T. Structural coherency of graphene on Ir(111). Nano Lett. 2008;8:565–70. DOI: 10.1021/nl0728874

[2] Sutter PW, Flege JI, Sutter EA. Epitaxial graphene on ruthenium. Nat Mater. 2008;7:406–11. DOI:10.1038/nmat2166

[3] Kim KS. Large-scale pattern growth of graphene films for stretchable transparent electrodes. Nature. 2009;457:706–10. DOI:10.1038/nature07719

[4] Berger C, Song Z, Li T, Li X, Ogbazghi AY, Feng R, et al. Ultrathin epitaxial graphite: 2D electron gas properties and a route toward graphene-based nanoelectronics. J Phys Chem B. 2004;108:19912–6. DOI: 10.1021/jp040650f

[5] Geim A, Novoselov K. The rise of graphene. Nat Mater. 2007;6:183–91. DOI:10.1038/nmat1849

[6] Shukla A, Kumar R, Mazher J, Balan A. Graphene made easy: High quality, large-area samples. Solid State Commun. 2009;149:718–21. DOI:http://dx.doi.org/10.1016/j.ssc.2009.02.007

[7] Park S, Ruoff RS. Chemical methods for the production of graphenes. Nat Nano. 2009;4:217–24. DOI:10.1038/nnano.2009.58

[8] Cai M, Thorpe D, Adamson DH, Schniepp HC. Methods of graphite exfoliation. J Mater Chem. 2012;22:24992–5002. DOI: 10.1039/c2jm34517j

[9] Brodie BC. On the atomic weight of graphite. Philos Trans R Soc Lond. 1859;149:249–59. DOI: 10.2307/108699

[10] Staudenmaier L. Verfahren zur Darstellung der Graphitsäure. Ber. Dtsch. Chem. Ges. 1898;31: 1481–1487. DOI: 10.1002/cber.18980310237

[11] Hummers W, Ofeman R. Preparation of graphitic oxide. J Am Chem Soc. 1958;80:1339. DOI: 10.1021/ja01539a017

[12] Vaisman L, Wagner HD, Marom G. The role of surfactants in dispersion of carbon nanotubes. Adv Colloid Interface Sci. 2006;128–130:37–46. DOI: http://dx.doi.org/10.1016/j.cis.2006.11.007

[13] Rajalakshmi N, Ryu H, Shaijumon MM, Ramaprabhu S. Performance of polymer electrolyte membrane fuel cells with carbon nanotubes as oxygen reduction catalyst support material. J Power Sources. 2005;140:250–7. DOI: 10.1016/j.jpowsour.2004.08.042

[14] Georgakilas V, Otyepka M, Bourlinos AB, Chandra V, Kim N, Kemp KC, et al. Functionalization of graphene: covalent and non-covalent approaches, derivatives and applications. Chem Rev (Washington, DC, USA). 2012;112:6156–214. DOI: 10.1021/cr3000412

[15] Andrews R, Jacques D, Qian D, Rantell T. Multiwall carbon nanotubes: synthesis and application. Acc Chem Res. 2002;35:1008–17. DOI: 10.1021/ar010151m

[16] Wu G, Li L, Li J-H, Xu B-Q. Methanol electrooxidation on Pt particles dispersed into PANI/SWNT composite films. J Power Sources. 2006;155:118–27. DOI: http://dx.doi.org/10.1016/j.jpowsour.2005.04.035

[17] Matarredona O, Rhoads H, Li Z, Harwell JH, Balzano L, Resasco DE. Dispersion of single-walled carbon nanotubes in aqueous solutions of the anionic surfactant NaDDBS. J Phys Chem B. 2003;107:13357–67. DOI: 10.1021/jp0365099

[18] Katz E, Willner I. Biomolecule-functionalized carbon nanotubes: applications in nanobioelectronics. ChemPhysChem. 2004;5:1084–104. DOI:10.1002/cphc.200400193

[19] Wang H, Maiyalagan T, Wang X. Review on recent progress in nitrogen-doped graphene: synthesis, characterization, and its potential applications. ACS Catal. 2012;2:781–94. DOI: 10.1021/cs200652y

[20] Winter M, Brodd RJ. What are batteries, fuel cells, and supercapacitors? Chem Rev (Washington, DC, USA). 2004;104:4245–70. DOI: 10.1021/cr020730k

[21] Gasteiger HA, Kocha SS, Sompalli B, Wagner FT. Activity benchmarks and requirements for Pt, Pt-alloy, and non-Pt oxygen reduction catalysts for PEMFCs. Appl Catal B: Environ. 2005;56:9–35. DOI: 10.1016/j.apcatb.2004.06.021

[22] Gröger O, Gasteiger HA, Suchsland J-P. Review—electromobility: batteries or fuel cells? J Electrochem Soc. 2015;162:A2605–A22. DOI: 10.1149/2.0211514jes

[23] Stamenkovic VR, Mun BS, Arenz M, Mayrhofer KJJ, Lucas CA, Wang G, et al. Trends in electrocatalysis on extended and nanoscale Pt-bimetallic alloy surfaces. Nat Mater. 2007;6:241–7. DOI:10.1038/nmat1840

[24] Toda T, Igarashi H, Uchida H, Watanabe M. Enhancement of the electroreduction of oxygen on Pt alloys with Fe, Ni, and Co. J Electrochem Soc. 1999;146:3750–6. DOI: 10.1149/1.1392544

[25] Vinayan BP, Ramaprabhu S. Platinum-TM (TM = Fe, Co) alloy nanoparticles dispersed nitrogen doped (reduced graphene oxide-multiwalled carbon nanotube) hybrid

structure cathode electrocatalysts for high performance PEMFC applications. Nanoscale. 2013;5:5109–18. DOI: 10.1039/c3nr00585b

[26] Vinayan BP, Nagar R, Rajalakshmi N, Ramaprabhu S. Novel platinum–cobalt alloy nanoparticles dispersed on nitrogen-doped graphene as a cathode electrocatalyst for PEMFC applications. Adv Funct Mater. 2012;22:3519–26. DOI: 10.1002/adfm.201102544

[27] Vinayan BP, Jafri RI, Nagar R, Rajalakshmi N, Sethupathi K, Ramaprabhu S. Catalytic activity of platinum–cobalt alloy nanoparticles decorated functionalized multiwalled carbon nanotubes for oxygen reduction reaction in PEMFC. Int J Hydrogen Energy. 2012;37:412–21. DOI: http://dx.doi.org/10.1016/j.ijhydene.2011.09.069

[28] Wang C, Markovic NM, Stamenkovic VR. Advanced platinum alloy electrocatalysts for the oxygen reduction reaction. ACS Catal. 2012;2:891–8. DOI: 10.1021/cs3000792

[29] Stephens IEL, Bondarenko AS, Gronbjerg U, Rossmeisl J, Chorkendorff I. Understanding the electrocatalysis of oxygen reduction on platinum and its alloys. Energy Environ Sci. 2012;5:6744–62. DOI: 10.1039/C2EE03590A

[30] Wu J, Yuan XZ, Martin JJ, Wang H, Zhang J, Shen J, et al. A review of PEM fuel cell durability: degradation mechanisms and mitigation strategies. J Power Sources. 2008;184:104–19. DOI:10.1016/j.jpowsour.2008.06.006

[31] Jafri RI, Arockiados T, Rajalakshmi N, Ramaprabhu S. Nanostructured Pt dispersed on graphene-multiwalled carbon nanotube hybrid nanomaterials as electrocatalyst for PEMFC. J Electrochem Soc. 2010;157:B874–B9. DOI: 10.1149/2.097311jes

[32] Seger B, Kamat PV. Electrocatalytically Active graphene-platinum nanocomposites. Role of 2-D carbon support in PEM fuel cells. J Phys Chem C. 2009;113:7990–5. DOI: 10.1021/jp900360k

[33] Li Y, Tang L, Li J. Preparation and electrochemical performance for methanol oxidation of pt/graphene nanocomposites. Electrochem Commun. 2009;11:846–9. DOI: 10.1016/j.elecom.2009.02.009

[34] Si Y, Samulski ET. Exfoliated graphene separated by platinum nanoparticles. Chem Mater. 2008;20:6792–7. DOI: 10.1021/cm801356a

[35] Zhu C, Dong S. Recent progress in graphene-based nanomaterials as advanced electrocatalysts towards oxygen reduction reaction. Nanoscale. 2013;5:1753–67. DOI: 10.1039/c2nr33839d

[36] Vinayan BP, Nagar R, Ramaprabhu S. Synthesis and investigation of mechanism of platinum–graphene electrocatalysts by novel co-reduction techniques for proton exchange membrane fuel cell applications. J Mater Chem. 2012;22:25325–34. DOI: 10.1039/C2JM33894G

[37] Vinayan BP, Nagar R, Raman V, Rajalakshmi N, Dhathathreyan KS, Ramaprabhu S. Synthesis of graphene-multiwalled carbon nanotubes hybrid nanostructure by

strengthened electrostatic interaction and its lithium ion battery application. J Mater Chem. 2012;22:9949–56. DOI: 10.1039/C2JM16294F

[38] Vinayan BP, Diemant T, Behm RJ, Ramaprabhu S. Iron encapsulated nitrogen and sulfur co-doped few layer graphene as a non-precious ORR catalyst for PEMFC application. RSC Adv. 2015;5:66494–501. DOI: 10.1039/C5RA09030J

[39] Vinayan BP, Schwarzburger NI, Fichtner M. Synthesis of a nitrogen rich (2D-1D) hybrid carbon nanomaterial using a $MnO_2$ nanorod template for high performance Li-ion battery applications. J Mater Chem A. 2015;3:6810–8. DOI: 10.1039/C4TA05642F

[40] Vinayan BP, Zhao-Karger Z, Diemant T, Chakravadhanula VSK, Schwarzburger NI, Cambaz MA, et al. Performance study of magnesium-sulfur battery using a graphene based sulfur composite cathode electrode and a non-nucleophilic Mg electrolyte. Nanoscale. 2016;8:3296–306. DOI: 10.1039/C5NR04383B

[41] Vinayan BP, Sethupathi K, Ramaprabhu S. Facile synthesis of triangular shaped palladium nanoparticles decorated nitrogen doped graphene and their catalytic study for renewable energy applications. Int J Hydrogen Energy. 2013;38:2240–50. DOI: http://dx.doi.org/10.1016/j.ijhydene.2012.11.091

[42] Sahoo M, Sreena KP, Vinayan BP, Ramaprabhu S. Green synthesis of boron doped graphene and its application as high performance anode material in Li ion battery. Mater Res Bull. 2015;61:383–90. DOI: http://dx.doi.org/10.1016/j.materresbull.2014.10.049

[43] Shin J, Choi J-H, Cha P-R, Kim SK, Kim I, Lee S-C, et al. Catalytic activity for oxygen reduction reaction on platinum-based core-shell nanoparticles: all-electron density functional theory. Nanoscale. 2015;7:15830–9. DOI: 10.1039/C5NR04706D

[44] Stamenkovic VR, Fowler B, Mun BS, Wang G, Ross PN, Lucas CA, et al. Improved oxygen reduction activity on Pt3Ni(111) via increased surface site availability.Science. 2007;315:493–7. DOI: 10.1126/science.1135941

[45] van der Vliet DF, Wang C, Tripkovic D, Strmcnik D, Zhang XF, Debe MK, et al. Mesostructured thin films as electrocatalysts with tunable composition and surface morphology. Nat Mater. 2012;11:1051–8. DOI:10.1038/nmat3457

[46] Geng D, Chen Y, Chen Y, Li Y, Li R, Sun X, et al. High oxygen-reduction activity and durability of nitrogen-doped graphene. Energy Environ Sci. 2011;4:760–4. DOI: 10.1039/C0EE00326C

[47] Zhou Y, Neyerlin K, Olson TS, Pylypenko S, Bult J, Dinh HN, et al. Enhancement of Pt and Pt-alloy fuel cell catalyst activity and durability via nitrogen-modified carbon supports. Energy Environ Sci. 2010;3:1437–46. DOI: 10.1039/C003710A